

# Infrared Spectra of Size Selected $\text{Cl}^-(\text{D}_2)_n$ and $\text{F}^-(\text{D}_2)_n$ Anion Clusters

D. A. Wild, P. S. Weiser, Z. M. Loh, and E. J. Bieske\*

School of Chemistry, University of Melbourne, Parkville 3010, Victoria, Australia

Received: July 26, 2001; In Final Form: November 12, 2001

Infrared vibrational predissociation spectra are reported for size-selected  $\text{F}^-(\text{D}_2)_n$  ( $n = 1-6$ ) and  $\text{Cl}^-(\text{D}_2)_n$  ( $n = 1-3$ ) clusters in the D–D stretch region. The  $\text{F}^-(\text{D}_2)_n$  and  $\text{Cl}^-(\text{D}_2)_n$  spectra each feature a single band shifted to lower energy from the bare  $\text{D}_2$  stretching frequency that moves to higher frequency with increasing cluster size. Vibrational band shifts are substantially larger for  $\text{F}^-(\text{D}_2)_n$  than for  $\text{Cl}^-(\text{D}_2)_n$ , reflecting the stronger  $\text{F}^--\text{D}_2$  interaction. The spectra are compatible with the  $\text{F}^-(\text{D}_2)_n$  and  $\text{Cl}^-(\text{D}_2)_n$  clusters containing roughly equivalent  $\text{D}_2$  ligands that are attached end-on to a central halide anion core. The unobserved D–D stretch band of the  $\text{F}^--\text{D}_2$  complex is predicted to lie at  $\sim 2400\text{ cm}^{-1}$ .

## 1. Introduction

Investigations of charged clusters comprising an ion surrounded by neutral ligands provide fundamental information on the intermolecular interactions responsible for ion solvation. Recently, different groups have set about exploring solvation effects in negatively charged complexes and clusters by recording and analyzing their infrared spectra. Most of the studies have focused on complexes comprising halide anions bonded to hydrogen containing ligands including  $\text{X}^-(\text{H}_2\text{O})_n$  ( $\text{X} = \text{F}, \text{Cl}, \text{Br}, \text{I}$ ),<sup>1–6</sup>  $\text{X}^-(\text{C}_2\text{H}_2)_n$  ( $\text{X} = \text{Cl}, \text{Br}, \text{I}$ ),<sup>7–9</sup>  $\text{Cl}^-(\text{CH}_3\text{OH})_n$ ,<sup>10</sup>  $\text{Cl}^-\text{NH}_3$ ,<sup>11</sup>  $\text{Cl}^-\text{CH}_4$ ,<sup>12</sup> and  $\text{Cl}^-\text{H}_2$ .<sup>13,14</sup> In many cases, cluster structures have been inferred from the frequencies of the hydrogen stretch bands, which depend sensitively upon the ligands' local environment. Vibrationally resolved infrared spectra have been used to elucidate: (1) the disposition of the ligands around the ion core; (2) the number of ligands that can be accommodated in the first solvation shell; and (3) whether secondary, ligand–ligand bonds play a significant role in determining the cluster structures.

The current work involves infrared spectroscopic investigations of size-selected  $\text{Cl}^-(\text{D}_2)_n$  and  $\text{F}^-(\text{D}_2)_n$  clusters in the D–D stretch region. Previously, complexes consisting of a halide anion attached to  $\text{H}_2$ , HD, or  $\text{D}_2$  ligands have been characterized in theoretical studies of  $\text{F}^-\text{H}_2$  and  $\text{F}^-\text{D}_2$ ,<sup>15–17</sup> photoelectron studies of  $\text{F}^-\text{H}_2$ ,<sup>18</sup>  $\text{F}^-\text{HD}$ ,<sup>19</sup> and  $\text{F}^-\text{D}_2$ ,<sup>19</sup> and infrared spectroscopic studies of  $\text{Cl}^-\text{H}_2$ ,<sup>13</sup>  $\text{Cl}^-\text{D}_2$ ,<sup>14</sup> and  $\text{Br}^-\text{D}_2$ .<sup>20</sup> To our knowledge, the current work is the first to address the properties of the larger clusters. Compared to anion clusters that feature extensive solvent networking (such as the hydrated halides), the  $\text{Cl}^-(\text{D}_2)_n$  and  $\text{F}^-(\text{D}_2)_n$  clusters should be relatively simple systems. The dominant cohesive forces are expected to arise from charge–quadrupole and charge-induced dipole interactions between the halide anion and the  $\text{D}_2$  ligands, both of which favor linear intermolecular bonds. Intermolecular interactions between  $\text{D}_2$  molecules are anticipated to play a minor cohesive role.

## 2. Experimental Methods

Vibrational predissociation spectra of the  $^{35}\text{Cl}^-(\text{D}_2)_n$  and  $\text{F}^-(\text{D}_2)_n$  complexes were recorded using a low energy guided

ion beam apparatus.<sup>7,9</sup> The machine consists of a cluster ion source, primary quadrupole mass filter for selection of the parent  $\text{X}^-(\text{D}_2)_n$  complexes, a quadrupole bender that deflects the beam through  $90^\circ$  into a 60 cm long octopole ion guide, a secondary quadrupole mass filter for selection of the photofragment, and an ion detector. During their passage through the octopole guide, the ions encounter a counter-propagating IR beam, which when tuned to an appropriate wavelength, serves to excite the complexes to predissociative vibrational levels, resulting in the production of charged photofragments. Spectra were measured by monitoring the fragment ion intensity as the wavelength of the infrared excitation light was scanned.

The  $^{35}\text{Cl}^-(\text{D}_2)_n$  and  $\text{F}^-(\text{D}_2)_n$  complexes were synthesized in an electron beam crossed supersonic expansion. A 1:100 mixture of  $\text{D}_2/\text{Ar}$  (8 bar) seeded with traces of either  $\text{CCl}_4$  (for  $\text{Cl}^-(\text{D}_2)_n$ ) or  $\text{NF}_3$  (for  $\text{F}^-(\text{D}_2)_n$ ) was expanded from a pulsed nozzle (0.8 mm orifice diameter, 40 Hz repetition rate) and crossed by 200 eV electrons issuing from twin rhenium filaments. The  $\text{Cl}^-$  and  $\text{F}^-$  anions were presumably formed through dissociative electron attachment to  $\text{CCl}_4$  and  $\text{NF}_3$ , respectively. The source design permits variation of the distance between the electron impact zone and nozzle orifice to maximize cluster production. Relatively small separations (1–2 mm) were found to favor  $\text{Cl}^-(\text{D}_2)_n$  and  $\text{F}^-(\text{D}_2)_n$  production, suggesting a formation mechanism whereby the  $\text{D}_2$  ligands accrete about halide anions through three body association processes in the early part of the supersonic expansion.

Tunable infrared light was produced using a Nd:YAG pumped optical parametric oscillator (OPO) capable of generating light in the  $2500\text{--}6900\text{ cm}^{-1}$  range with a bandwidth of  $\sim 0.017\text{ cm}^{-1}$ . Wavelength calibration was accomplished using a wavemeter (New Focus 7711), through measurements of the OPO oscillator wavelength and the 532 nm output of the seeded Nd:YAG laser. The pulsed ion source was run at twice the repetition rate of the laser so that laser on/off background subtraction could be used to account for collisional and metastable fragmentation.

Absorption of a single infrared photon in the  $2500\text{--}3000\text{ cm}^{-1}$  range should provide the  $\text{F}^-(\text{D}_n)_n$  and  $\text{Cl}^-(\text{D}_2)_n$  clusters with sufficient energy to shed at least one  $\text{D}_2$  ligand. The energetic cost of removing a single  $\text{D}_2$  ligand is expected to be largest for  $\text{F}^-\text{D}_2$ . Although there are no experimental mea-

\* To whom correspondence should be addressed. E-mail: evanj@unimelb.edu.au.

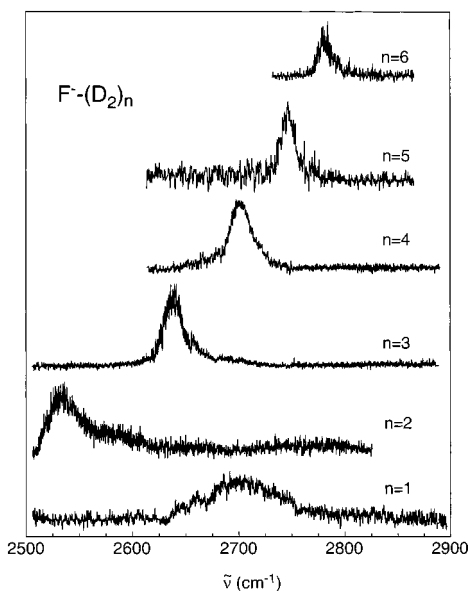


**Figure 1.** Mid-infrared vibrational predissociation spectra of mass selected  $\text{F}^-(\text{D}_2)_n$  ( $1 \leq n \leq 6$ ) clusters in the 2500–2900  $\text{cm}^{-1}$  range (D–D stretch region). Table 1 lists the band positions, widths, and shifts with respect to the free  $\text{D}_2$  stretch frequency.

**TABLE 1: Band Positions, Vibrational Band Shifts, and Estimated Band Widths for the  $\text{F}^-(\text{D}_2)_n$  ( $n = 1-6$ ) and  $^{35}\text{Cl}^-(\text{D}_2)_n$  ( $n = 1-3$ ) Clusters<sup>a</sup>**

| cluster                           | band position ( $\text{cm}^{-1}$ ) | band shift ( $\text{cm}^{-1}$ ) | width ( $\text{cm}^{-1}$ ) |
|-----------------------------------|------------------------------------|---------------------------------|----------------------------|
| $\text{F}^-\text{D}_2$            | 2700(15)                           | −294                            | 80                         |
| $\text{F}^-(\text{D}_2)_2$        | 2537(10)                           | −457                            | 40                         |
| $\text{F}^-(\text{D}_2)_3$        | 2637(7)                            | −357                            | 30                         |
| $\text{F}^-(\text{D}_2)_4$        | 2706(7)                            | −288                            | 25                         |
| $\text{F}^-(\text{D}_2)_5$        | 2750(5)                            | −244                            | 20                         |
| $\text{F}^-(\text{D}_2)_6$        | 2780(5)                            | −214                            | 18                         |
| $\text{Cl}^-\text{D}_2(p)$        | 2878.75(8)                         | −114.8                          | N/A                        |
| $\text{Cl}^-\text{D}_2(o)$        | 2878.51(8)                         | −113.0                          | N/A                        |
| $\text{Cl}^-\text{D}_2\text{-Ar}$ | 2880(5)                            | −114                            | 18                         |
| $\text{Cl}^-(\text{D}_2)_2$       | 2887(5)                            | −107                            | 22                         |
| $\text{Cl}^-(\text{D}_2)_3$       | 2891(5)                            | −103                            | 18                         |

<sup>a</sup> The vibrational band shift for  $\text{Cl}^-\text{D}_2(o)$  is given with respect to the  $\text{Q}_1(1)$  transition of the free  $\text{D}_2$  molecule ( $2991.46 \text{ cm}^{-1}$ , ref 21). Shifts for other bands are given with respect to the  $\text{Q}_1(0)$  transition of the free  $\text{D}_2$  molecule ( $2993.57 \text{ cm}^{-1}$ , ref 21). Estimated uncertainties in the last significant figure are given in parentheses.

measurements for the binding energy of this species, ab initio and rovibrational calculations predict  $D_0 = 1560 \text{ cm}^{-1}$  for the related  $\text{F}^-\text{H}_2$  isotopomer.<sup>17</sup> The dissociation energy for  $\text{F}^-\text{D}_2$  should be slightly larger, due to its lower zero point vibrational energy, though it is unlikely to exceed  $2500 \text{ cm}^{-1}$ . The binding energy is expected to diminish as the clusters become larger, and for equivalent cluster size should be less for  $\text{Cl}^-(\text{D}_2)_n$  than  $\text{F}^-(\text{D}_2)_n$ .

### 3. Results and Discussion

**3.1. Spectra of  $\text{F}^-(\text{D}_2)_n$ .** Infrared spectra of the  $\text{F}^-(\text{D}_2)_n$  complexes ( $n = 1-6$ ), recorded over the 2500–2900  $\text{cm}^{-1}$  range, are shown in Figure 1. Scans for the  $n = 1-4$  clusters were recorded by monitoring the  $\text{F}^-(\text{D}_2)_{n-1}$  dissociation channel, whereas the  $n = 5$  & 6 cluster spectra were recorded by monitoring the  $\text{F}^-(\text{D}_2)_{n-2}$  channel. Band wavenumbers, shifts with respect to the free  $\text{D}_2$  stretch vibration,<sup>21</sup> and widths are listed in Table 1.

The  $\text{F}^-(\text{D}_2)_n$ ,  $n = 2-6$  spectra each feature a single peak shifted to lower energy from the bare  $\text{D}_2$  stretching frequency

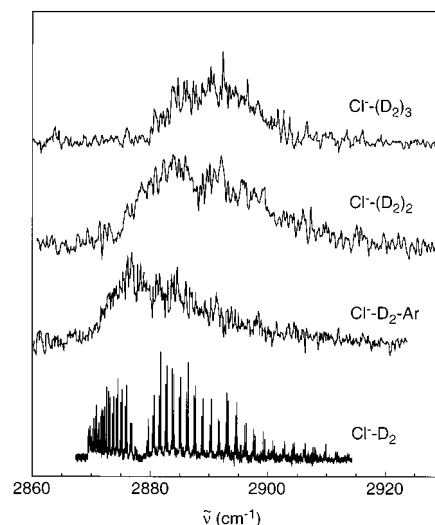


**Figure 2.** Mid-infrared vibrational predissociation spectra of mass selected  $^{35}\text{Cl}^-(\text{D}_2)_n$  ( $1 \leq n \leq 3$ ) clusters in the 2860–2920  $\text{cm}^{-1}$  range (D–D stretch region). Also shown is the spectrum of  $\text{Cl}^-\text{D}_2\text{-Ar}$ . Table 1 lists the band positions, widths, and shifts with respect to the free  $\text{D}_2$  stretch frequency.

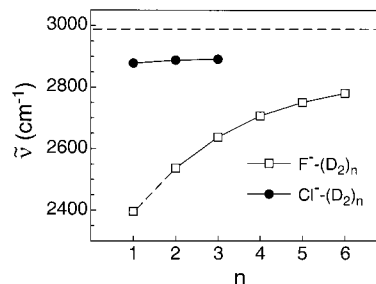


**Figure 3.** Frequency of the infrared active D–D stretch band for the  $^{35}\text{Cl}^-(\text{D}_2)_n$  and  $\text{F}^-(\text{D}_2)_n$  clusters versus ligand number. The dashed line corresponds to the vibrational frequency of the free  $\text{D}_2$  molecule.<sup>21</sup> The  $\text{F}^-\text{D}_2$  band position ( $2400 \text{ cm}^{-1}$ ) is estimated by extrapolating the  $\text{F}^-(\text{D}_2)_n$  ( $2 \leq n \leq 6$ ) data.

that moves steadily to higher energy with increasing cluster size. Oddly, the only observed band for  $\text{F}^-\text{D}_2$ , which lies at  $\sim 2700 \text{ cm}^{-1}$  approximately  $165 \text{ cm}^{-1}$  higher in energy than the  $\text{F}^-(\text{D}_2)_2$  peak, does not fit the general trend. The most likely explanation for this apparent irregularity is that the  $2700 \text{ cm}^{-1}$  band of  $\text{F}^-\text{D}_2$  is associated with the D–D stretch mode in combination with the intermolecular stretch mode (i.e.,  $\nu_{\text{DD}} + \nu_s$ ), and that the  $\nu_{\text{DD}}$  fundamental lies below  $2500 \text{ cm}^{-1}$ , outside the range of the OPO system. If the  $2700 \text{ cm}^{-1}$  band is indeed the  $\nu_{\text{DD}} + \nu_s$  transition, then the frequency of the  $\nu_{\text{DD}}$  fundamental can be estimated as  $\sim 2460 \text{ cm}^{-1}$  using the  $\nu_s$  frequency of  $243 \text{ cm}^{-1}$  calculated by Boldyrev et. al.<sup>16</sup> This estimate agrees reasonably well with the value of  $2400 \text{ cm}^{-1}$  obtained by extrapolating the band positions for the  $n = 2-6$  clusters.

**3.2. Spectra of  $\text{Cl}^-(\text{D}_2)_n$ .** Vibrational predissociation spectra for the  $\text{Cl}^-(\text{D}_2)_n$  ( $n = 1-3$ ) complexes, recorded over the 2860–2920  $\text{cm}^{-1}$  range, are shown in Figure 2. As in the case of  $\text{F}^-(\text{D}_2)_n$ , each of the  $\text{Cl}^-(\text{D}_2)_n$  spectra features a single band that can be readily assigned to the D–D stretch vibration of the  $\text{D}_2$  ligand(s). Band wavenumbers, shifts with respect to the free  $\text{D}_2$  stretch vibration,<sup>21</sup> and widths are given in Table 1. Frequencies for the band maxima (along with those of  $\text{F}^-(\text{D}_2)_n$ ) are plotted as a function of cluster size in Figure 3. It can be seen that the frequency of the  $\text{Cl}^-(\text{D}_2)_n$  band increases steadily

with cluster size, although the variation is less dramatic than that of the  $F^-(D_2)_n$  series.

The band of  $Cl^-(D_2)$  (Figure 2) exhibits rotationally resolved features and comprises two overlapping  $\Sigma-\Sigma$  subbands (separated by  $0.24\text{ cm}^{-1}$ ) that arise from complexes containing *para* and *ortho*  $D_2$  molecules. The rotational structure of the band is compatible with  $Cl^-(D_2)$  possessing a linear equilibrium geometry (although zero-point bending and stretching motions are expected to be substantial). Analysis of the spectrum is detailed in an earlier publication where rotational constants ( $B$  and  $D$  values) are reported for the ground and excited states.<sup>14</sup> The rotational constants are consistent with a vibrationally averaged  $Cl^- \cdots D_2$  intermolecular separation of  $3.16\text{ \AA}$ , contracting by  $0.08\text{ \AA}$  when the D-D stretch mode is excited. The bond contraction (which is reflected in the prominent P-branch head) can be attributed to increases in the  $D_2$  quadrupole moment and polarizabilities in the vibrationally excited state. The binding energies of *para* and *ortho*  $D_2$  to  $Cl^-$  have been estimated as  $499$  and  $559\text{ cm}^{-1}$ , on the basis of potential energy curves developed by RKR inversion of the rotational constants and consideration of the long-range induction and electrostatic interaction between the  $Cl^-$  and  $D_2$  subunits.<sup>14</sup>

**3.3. Cluster Structures.** The available data suggest that the  $F^-(D_2)_n$  and  $Cl^-(D_2)_n$  clusters should be essentially comprised of intact  $D_2$  subunits attached to the halide anions by electrostatic and induction forces. The proton affinity of  $H^-$  ( $1675\text{ kJ/mol}$ <sup>22</sup>) considerably exceeds those of  $F^-$  ( $1554.8\text{ kJ/mol}$ <sup>23</sup>) and  $Cl^-$  ( $1395\text{ kJ/mol}$ <sup>24</sup>), so that deuteron transfer to the halide anions should not seriously disrupt the structural integrity of the  $D_2$  molecules. The dominant cohesive forces responsible for stability of the  $F^-(D_2)_n$  and  $Cl^-(D_2)_n$  clusters are expected to arise from charge-quadrupole and charge-induced dipole interactions between the  $D_2$  ligands and the halide anion. Both of these interactions favor linear intermolecular bonds. Support for a linear equilibrium structure for the halide anion- $H_2$  complexes comes from ab initio calculations for  $F^-H_2$ ,<sup>15-17</sup> and rotationally resolved IR spectra of  $Cl^-H_2$ ,<sup>13</sup>  $Cl^-(D_2)$ ,<sup>14</sup> and  $Br^-(D_2)$ .<sup>20</sup> In the larger  $Cl^-(D_2)_n$  and  $F^-(D_2)_n$  clusters,  $D_2$  ligands that are arranged such that their bonds are aligned with a central halide anion, are expected to avoid one another due to repulsive quadrupole-quadrupole interactions reinforced by repulsive interactions between the dipoles induced by the anion's charge. For this reason, it is anticipated that the  $X^-(D_2)_n$  clusters should possess interior solvation structures in which the  $D_2$  ligands are disposed about a central halide anion core.

Equilibrium cluster structures that contain equivalent or near-equivalent  $D_2$  ligands that are bonded end-on to a central halide anion and which are best positioned to avoid one another are similar to those commonly encountered for inorganic transition metal complexes. As shown in Figure 4, the  $X^-(D_2)_2$  complex is postulated to be linear,  $X^-(D_2)_3$  trigonal planar,  $X^-(D_2)_4$  tetrahedral,  $X^-(D_2)_5$  trigonal bipyramidal, and  $X^-(D_2)_6$  octahedral. The clusters are expected to be extremely floppy, undergoing substantial zero point excursions, particularly in vibrational modes corresponding to angular motion of the ligands' centers of mass about the central anion core, and hindered internal rotation of the  $D_2$  subunits.

To estimate the importance of the ligand-ligand repulsive interactions, the quadrupole-quadrupole, induced dipole-induced dipole and induced dipole-permanent quadrupole interaction energies were estimated for two adjacent  $D_2$  molecules in an octahedral complex (Figure 4(f)). The  $F^- \cdots D_2$

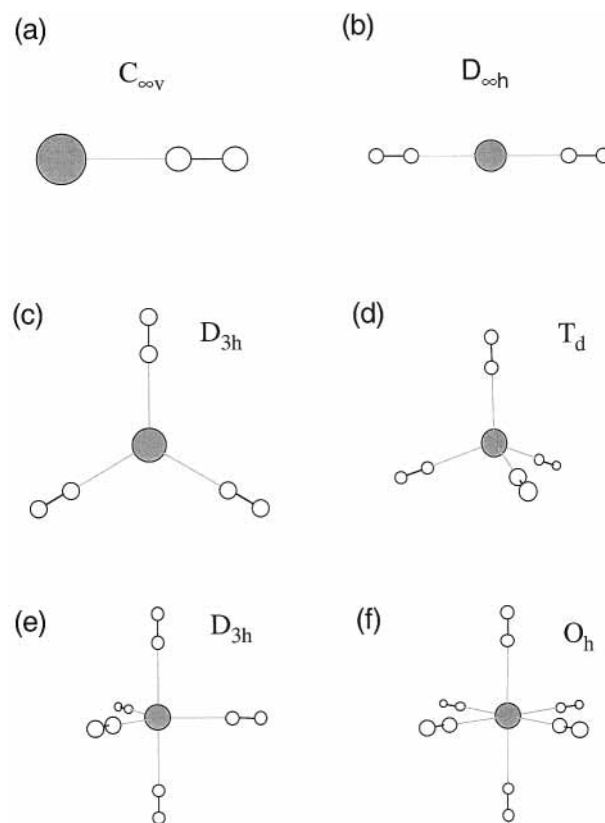


**Figure 4.** Postulated equilibrium structures for the  $X^-(D_2)_n$  clusters derived from consideration of the infrared spectra and the dominant ligand-ion and ligand-ligand interactions.

separation was taken from the ab initio  $F^-D_2$  equilibrium geometry of Boldyrev et al.<sup>16</sup> ( $R_{cm}=2.07\text{ \AA}$ ), whereas the experimental vibrationally averaged  $Cl^-D_2$  intermolecular bond length<sup>14</sup> ( $R_{cm}=3.16\text{ \AA}$ ) was used for the  $Cl^- \cdots D_2$  separation. The quadrupole moment and dipole polarizabilities of  $D_2$  necessary for the estimations were taken from reference 25. The induced dipole-induced dipole, induced dipole-quadrupole, and quadrupole-quadrupole energies are  $+365$ ,  $+156$ , and  $+35\text{ cm}^{-1}$  for the  $D_2-F^-D_2$  system and  $+19$ ,  $+12$ , and  $+4\text{ cm}^{-1}$  for the  $D_2-Cl^-D_2$  system. In this simple model, where the halide anion is represented as a point negative charge, the difference in the  $D_2-D_2$  interaction energies for the two systems is solely due to differences in the halide- $D_2$  and  $D_2-D_2$  bond lengths. Although several effects, such as the hindered internal rotation of the  $D_2$  ligands, have been ignored in the estimation of the  $D_2 \cdots D_2$  interaction energies, it seems obvious that the repulsive interactions are sufficient to overwhelm weak van der Waals attractions that might cause the  $D_2$  subunits to congregate.

The mid-infrared spectra of  $F^-(D_2)_n$  and  $Cl^-(D_2)_n$  (Figures 1 and 2) are consistent with the structures shown in Figure 4. The existence of a single mid-infrared band for each cluster size strongly suggests that the  $D_2$  ligands are similarly perturbed by the halide anion and are roughly equivalent to one another. The  $n = 1, 2, 3, 4$ , and  $6$  clusters shown in Figure 4 will possess only a single infrared active collective D-D stretch vibrational mode (doubly degenerate for  $n = 3$  and triply degenerate for  $n = 4$  and  $6$ ). In the case of  $F^-(D_2)_5$  the two inequivalent groups of  $D_2$  ligands (corresponding to axial and equatorial positions) will be associated with two infrared active stretch modes (one singly degenerate and the other doubly degenerate). However, the appearance in the  $F^-(D_2)_5$  spectrum of a single relatively narrow band (fwhm  $\sim 20\text{ cm}^{-1}$ ) suggests that the axial and equatorial  $D_2$  ligands are similarly perturbed by the central

fluoride anion. It is possible that the barrier for pseudorotational interconversion of axial and equatorial ligands is extremely low, perhaps lying below the zero point energy for the motion, rendering the 5 ligands effectively equivalent to one another.

For both the  $\text{F}^-(\text{D}_2)_n$  and  $\text{Cl}^-(\text{D}_2)_n$  series, the steady displacement of the mid-infrared band back toward the bare  $\text{D}_2$  stretching frequency with increasing cluster size, suggests that the intermolecular bonds linking the  $\text{D}_2$  molecules to the halide anion becomes progressively longer and weaker as more ligands are added. With the addition of each  $\text{D}_2$  subunit, repulsive ligand-ligand interactions will serve to expand the solvent shell, increasing the  $\text{X}^- \cdots \text{D}_2$  bond distances, and reducing the influence of the halide anion on the vibrational properties of the  $\text{D}_2$  ligands. The much larger changes in vibrational frequency for  $\text{F}^-(\text{D}_2)_n$  compared to  $\text{Cl}^-(\text{D}_2)_n$  accompanying addition of each  $\text{D}_2$  subunit are compatible with considerably greater ligand-ligand repulsions in the  $\text{F}^-$  containing clusters.

There is no evidence from the spectra of  $\text{F}^-(\text{D}_2)_n$  or  $\text{Cl}^-(\text{D}_2)_n$  that the point has been reached where the first solvation shell has been filled. In earlier IR studies of  $\text{Cl}^-(\text{C}_2\text{H}_2)_n$ <sup>7</sup> and  $\text{Br}^-(\text{C}_2\text{H}_2)_n$ ,<sup>8</sup> where interior solvation structures were inferred from the frequencies of the ligand acetylene  $\nu_3$  vibrations (the IR active antisymmetric C-H stretch), the onset of the second solvation shell was observed at  $n = 7-8$ , and was signaled by the presence of a weak band close to the  $\nu_3$  frequency of the free acetylene molecule (due to ligand(s) in the second solvation shell), and by the fact that the  $\nu_3$  frequency for ligands situated in the first shell reached an asymptote. The spectra of  $\text{F}^-(\text{D}_2)_n$  and  $\text{Cl}^-(\text{D}_2)_n$  show no evidence for peaks to higher energy that could be associated with ligands in the second solvent shell, although such peaks should be weak and their detection may be problematic because the  $\text{D}_2$  stretch mode is rendered infrared active largely by virtue of its interaction with the halide anion. Perhaps more pertinently, the D-D stretch frequency increases steadily with cluster size for both the  $\text{Cl}^-(\text{D}_2)_n$  and  $\text{F}^-(\text{D}_2)_n$  series up to  $n = 3$  and  $n = 6$  respectively, and in neither case shows signs of having reached an asymptote. At this stage, the evidence merely suggests that the first solvation shells of  $\text{Cl}^-(\text{D}_2)_n$  and  $\text{F}^-(\text{D}_2)_n$  can accommodate at least 3 and 6  $\text{D}_2$  molecules, respectively. Infrared studies of yet larger complexes along with theoretical work may resolve the issue.

**3.4. Vibrational Band Profiles.** Only the  $\text{Cl}^-\text{D}_2$  spectrum exhibits resolved rotational structure with the D-D stretch bands of the other clusters appearing as broad unresolved contours. Perhaps most surprising is that the infrared band of  $\text{F}^-\text{D}_2$  does not contain resolved rovibrational lines. This is despite the fact that the estimated rotational constant of  $\text{F}^-\text{D}_2$  ( $1.1 \text{ cm}^{-1}$ )<sup>16</sup> is far larger than the infrared light bandwidth ( $\sim 0.017 \text{ cm}^{-1}$ ). We can merely speculate that predissociation from the upper state is extremely rapid leading to substantial lifetime broadening of the rovibrational lines. Although the rovibrational lines of  $\text{Cl}^-\text{D}_2$  have widths ( $\sim 0.03 \text{ cm}^{-1}$ ) that are only slightly greater than the OPO bandwidth, it is conceivable that vibrational predissociation is more rapid for the upper level of  $\text{F}^-\text{D}_2$  accessed in this study. It is also possible that the  $\text{F}^-\text{D}_2$  band contour comprises a number of overlapping hot bands leading to spectral congestion.

Even for the larger clusters, the rotational constants should exceed the infrared light bandwidth. For example, assuming a trigonal planar structure with  $\text{Cl}^- \cdots \text{D}_2$  bond length of  $3.5 \text{ \AA}$ , the rotational constants of  $\text{Cl}^-(\text{D}_2)_3$  are  $A = B = 0.22 \text{ cm}^{-1}$  and  $C = 0.11 \text{ cm}^{-1}$ . Similarly, assuming an octahedral structure with  $\text{F}^- \cdots \text{D}_2$  bond length of  $2.5 \text{ \AA}$ , the rotational constants for  $\text{F}^-(\text{D}_2)_6$  are  $A = B = C = 0.16 \text{ cm}^{-1}$ . In addition to

lifetime broadening, other factors may conspire to obscure rotational structure in the larger clusters' spectra. First, the clusters will exist in different forms containing various combinations of *para* and *ortho*  $\text{D}_2$  molecules, each of which will have a slightly different infrared spectrum. This effect is clearly manifested in the spectrum of  $\text{Cl}^-\text{D}_2$  (Figure 1) where the subbands due to  $\text{Cl}^-\text{D}_2(p)$  and  $\text{Cl}^-\text{D}_2(o)$  are separated by  $0.24 \text{ cm}^{-1}$ . In future, it may be possible to eliminate this source of congestion by manufacturing the clusters from pure *para*  $\text{D}_2$ . Second, as mentioned above, the presence of overlapping hot bands may contribute to spectral congestion. Clusters containing multiple  $\text{D}_2$  ligand should be extremely floppy, particularly in the lower frequency bending motions, so that the fundamental transition will almost inevitably be overlapped by hot bands.

The contours of the D-D stretch bands of  $\text{F}^-(\text{D}_2)_n$  and  $\text{Cl}^-(\text{D}_2)_n$  become noticeably narrower and more symmetric as the clusters become larger (Table 1). The effects are most obvious for the  $\text{F}^-(\text{D}_2)_n$  series (Figure 2). For example, the  $\text{F}^-(\text{D}_2)_2$  band has a pronounced high energy tail and  $\sim 40 \text{ cm}^{-1}$  width, whereas the corresponding  $\text{F}^-(\text{D}_2)_6$  band is almost symmetrical and has a width of  $\sim 18 \text{ cm}^{-1}$ . Similar trends have been discerned in IR spectra of  $\text{Cl}^-(\text{C}_2\text{H}_2)_n$ <sup>7</sup> and  $\text{Br}^-(\text{C}_2\text{H}_2)_n$ .<sup>8</sup> The vibrational band narrowing is accounted for, at least in part, by the smaller rotational constants of the larger clusters. Another significant influence on the bands' widths and asymmetries is related to a diminishing displacement of hot bands from the fundamental  $\nu_{\text{DD}}$  transition as the clusters become larger. Hot bands of the type  $\nu_{\text{DD}} + n\nu_s - n\nu_b$  and  $\nu_{\text{DD}} + n\nu_b - n\nu_s$  (where  $\nu_s$  and  $\nu_b$  are intermolecular stretching and bending modes) are expected to be shifted to higher energy from the fundamental  $\nu_{\text{DD}}$  transition because the intermolecular bonds should contract and stiffen when D-D stretch modes are excited (due to increases in the quadrupole moment and polarizabilities of  $\text{D}_2$  in the vibrationally excited state<sup>25</sup>). With increasing cluster size, the intermolecular bonds become progressively longer and weaker, reducing the effect of the  $\text{D}_2$  stretch mode on the intermolecular potential, and diminishing the offset of the hot bands from the  $\nu_{\text{DD}}$  fundamental.

**3.5. Spectrum of the  $\text{Cl}^-\text{D}_2\text{-Ar}$  Complex.** The infrared spectrum of  $\text{Cl}^-\text{D}_2\text{-Ar}$  (Figure 2) was measured in an effort to gauge the effect of argon solvation on the  $\text{Cl}^-\text{D}_2$  complex. The spectrum, which was obtained by monitoring the  $\text{Cl}^-\text{Ar}$  photofragment, features a single band that retains the asymmetric, blue-degraded form of the  $\text{Cl}^-\text{D}_2$  spectrum. Although it is difficult to locate the band's origin exactly (due to its width and poor signal-to-noise ratio), it appears that addition of an Ar atom has a minimal effect on the D-D stretch vibrational mode of  $\text{Cl}^-\text{D}_2$  and that the Ar solvent induced vibrational shift is small ( $< 5 \text{ cm}^{-1}$ ). The shift is comparable with those observed for argon-solvated hydrated halide clusters where the band shift is  $\sim 3 \text{ cm}^{-1}/\text{Ar}$  atom for  $\text{I}^-(\text{H}_2\text{O})(\text{Ar})_n$ <sup>26</sup> and even less for  $\text{Cl}^-(\text{H}_2\text{O})(\text{Ar})_n$ .<sup>6</sup>

There are interesting differences in the fragmentation pattern of  $\text{Cl}^-\text{D}_2\text{-Ar}$  following collisional excitation or photon absorption. Collision induced dissociation of  $\text{Cl}^-\text{D}_2\text{-Ar}$  by residual gas in the octopole ion guide produced approximately the same amounts of  $\text{Cl}^-\text{D}_2$  and  $\text{Cl}^-\text{Ar}$  fragments, consistent with the fact that the binding energies of  $\text{Cl}^-\text{Ar}$  ( $\sim 500 \text{ cm}^{-1}$ , reference 27) and  $\text{Cl}^-\text{D}_2$  ( $\sim 500 \text{ cm}^{-1}$ , reference 14) are similar. In contrast, as far as we could determine, IR excitation of the D-D stretch vibration in  $\text{Cl}^-\text{D}_2\text{-Ar}$  results exclusively in  $\text{Cl}^-\text{Ar}$  fragment ions. Although the energy of a single quantum of the  $\text{D}_2$  stretch vibration is more than sufficient to break the complex into  $\text{Cl}^- + \text{D}_2 + \text{Ar}$  fragments, it seems

that little of the available energy is transferred to the  $\text{Cl}^-$ -Ar bond. The observations are compatible with the D-D vibrational energy being transferred directly to the  $\text{Cl}^-$ -D<sub>2</sub> bond followed by prompt loss of the D<sub>2</sub>. Conservation of momentum and energy ensures that the light D<sub>2</sub> molecule departs with most of the excess energy, leaving insufficient energy to rupture the  $\text{Cl}^-$ -Ar bond.

#### 4. Conclusions and Outlook

The main conclusion of this work is that the smaller  $\text{F}^-(\text{D}_2)_n$  and  $\text{Cl}^-(\text{D}_2)_n$  clusters possess interior solvation structures such that the halide anion is surrounded by D<sub>2</sub> ligands that avoid one another due to repulsive electrostatic and three body interactions. There are several avenues for further work. First, it would be useful to measure IR spectra of larger  $\text{F}^-(\text{D}_2)_n$  and  $\text{Cl}^-(\text{D}_2)_n$  clusters to ascertain how many D<sub>2</sub> ligands can be accommodated in the first solvation shells of both species. It would also be interesting to investigate the  $\text{F}^-(\text{H}_2)_n$  and  $\text{Cl}^-(\text{H}_2)_n$  isotopomers to see whether the trends regarding band shifts are similar to those observed in this study. Clusters containing H<sub>2</sub> ligands should exhibit larger zero-point effects and lower binding energies than those containing D<sub>2</sub> ligands, and it is conceivable that this may reduce the number of ligands that can be situated in the inner solvation shell. Finally, it may be worthwhile pursuing the  $\nu_{\text{DD}}$  spectrum of  $\text{F}^-$ -D<sub>2</sub>, which the current study suggests lies at around 2400  $\text{cm}^{-1}$ , using alternative strategies such as direct laser absorption spectroscopy of complexes produced in an electron impact excited supersonic plasma.

**Acknowledgment.** The authors thank the Australian Research Council and the University of Melbourne for financial support.

#### References and Notes

- (1) Cabarcos, O. M.; Weinheimer, C. J.; Lisy, J. M.; Xantheas, S. S. *J. Chem. Phys.* **1999**, *110*, 5–8.
- (2) Choi, J.-H.; Kuwata, K. T.; Cao, Y.-B.; Okumura, M. *J. Phys. Chem.* **1998**, *102*, 503–507.

- (3) Ayotte, P.; Weddle, G. H.; Johnson, M. A. *J. Chem. Phys.* **1999**, *110*, 7129–7132.
- (4) Ayotte, P.; Bailey, C. G.; Weddle, G. H.; Johnson, M. A. *J. Phys. Chem.* **1998**, *102*, 3067–3071.
- (5) Johnson, M.; Kuwata, K.; Wong, C.; Okumura, M. *Chem. Phys. Lett.* **1996**, *260*, 551–557.
- (6) Kelley, J. A.; Weber, J. M.; Lisle, K. M.; Robertson, W. H.; Ayotte, P.; Johnson, M. A. *Chem. Phys. Lett.* **2000**, *327*, 1–6.
- (7) Weiser, P. S.; Wild, D. A.; Bieske, E. J. *J. Chem. Phys.* **1999**, *110*, 9443–9449.
- (8) Wild, D. A.; Milley, P. J.; Loh, Z. M.; Weiser, P. S.; Bieske, E. J. *Chem. Phys. Lett.* **2000**, *323*, 49–54.
- (9) Weiser, P. S.; Wild, D. A.; Bieske, E. J. *Chem. Phys. Lett.* **1999**, *299*, 303–308.
- (10) Cabarcos, O. M.; Weinheimer, C. J.; Martinez, T. J.; Lisy, J. M. *J. Chem. Phys.* **1999**, *110*, 9516–9526.
- (11) Weiser, P. S.; Wild, D. A.; Wolyneec, P.; Bieske, E. J. *J. Phys. Chem.* **2000**, *104*, 2562–2566.
- (12) Wild, D. A.; Loh, Z.; Wolyneec, P. P.; Weiser, P. S.; Bieske, E. J. *Chem. Phys. Lett.* **2000**, *332*, 531–537.
- (13) Wild, D. A.; Wilson, R. L.; Weiser, P. S.; Bieske, E. J. *J. Chem. Phys.* **2000**, *113*, 10 154.
- (14) Wild, D. A.; Weiser, P. S.; Bieske, E. J.; Zehnacker, A. *J. Chem. Phys.* **2001**, accepted.
- (15) Nichols, J. A.; Kendall, R. A.; Cole, S. J.; Simons, J. *J. Phys. Chem.* **1991**, *95*, 1074.
- (16) Boldyrev, A. I.; Simons, J.; Mil'nikov, G. V.; Benderskii, V. A.; Grebenshchikov, S. Y.; V. Vetoshkin, E. *J. Chem. Phys.* **1995**, *102*, 1295.
- (17) Hartke, B.; Werner, H.-J. *Chem. Phys. Lett.* **1997**, *280*, 430.
- (18) Weaver, A.; Metz, R. B.; Bradforth, S. E.; Neumark, D. M. *J. Chem. Phys.* **1990**, *93*, 5352–3.
- (19) Weaver, A.; Neumark, D. M. *Faraday Discuss. Chem. Soc.* **1991**, *91*, 5–16.
- (20) Wild, D. A.; Weiser, P. S.; Bieske, E. J. *J. Chem. Phys.* **2001**, *115*, 6394–6400.
- (21) Huber, K. P.; Herzberg, G. *Molecular Spectra and Molecular Structure IV. Constants of Diatomic Molecules*; van Nostrand Reinhold: New York, 1979.
- (22) Lykke, K. R.; Murray, K. K.; Lineberger, W. C. *Phys. Rev. A* **1991**, *43*, 6104.
- (23) Blondel, C.; Cacciani, P.; Delsart, C.; Trainham, R. *Phys. Rev. A* **1989**, *40*, 3698.
- (24) Martin, J. D. D.; Hepburn, J. W. *J. Chem. Phys.* **1998**, *109*, 8139–8142.
- (25) Hunt, J. L.; Poll, J. D.; Wolniewicz, L. *Can. J. Phys.* **1984**, *62*, 1719–23.
- (26) Ayotte, P.; Weddle, G. H.; Kim, J.; Kelley, J.; Johnson, M. A. *J. Phys. Chem. A* **1999**, *103*, 443–447.
- (27) Lenzer, T.; Yourshaw, I.; Furlanetto, M. R.; Reiser, G.; Neumark, D. M. *J. Chem. Phys.* **1999**, *110*, 9578–9586.